Hindawi
Shock and Vibration
Volume 2021, Article ID 6697682, 13 pages
https://doi.org/10.1155/2021/6697682

Research Article

A New Zoning Method of Blasting Vibration Based on Energy Proportion and Its SVM Classification Models

Haixia Wei,[1,2] Jinfeng Chen,[1] Jie Zhu,[1] Xiaolin Yang,[1] Huaibao Chu,[1] and Xisen Liu[1]

[1]*School of Civil Engineering, Henan Polytechnic University, Jiaozuo 454000, Henan, China*
[2]*Fujian Research Center for Tunneling and Urban Underground Space Engineering, Huaqiao University, Xiamen 361021, Fujian, China*

Correspondence should be addressed to Jinfeng Chen; 2283969514@qq.com

Received 21 October 2020; Revised 19 January 2021; Accepted 1 February 2021; Published 11 February 2021

Academic Editor: Fabio Minghini

The blasting vibration signals show obvious zoning propagation characteristics. Because of not considering the specific influences of geological and topographical conditions, the existing zoning methods of blasting vibration cannot fully describe the internal details of blasting vibration signals. Therefore, a new zoning method of blasting vibration based on energy proportion was proposed in this paper, in which the energy proportion in low, medium, and high frequency bands after multiresolution wavelet analysis is used as the zoning index to distinguish the different characteristics of blasting vibration signals in different zones. Based on the proposed zoning method, 343 sets of measured blasting vibration signals were used to train and test the SVM classification models with four different types of kernel functions. The testing results demonstrate that the zoning method of blasting vibration based on energy proportion has high feasibility, flexibility, and reliability, and the SVM classification models with RBF have higher accuracy than models with other kernel functions in blasting vibration zoning prediction.

1. Introduction

Blasting technology not only brings convenience to engineering construction but also causes a series of negative effects, among which blasting vibration effect is the most serious. Under the influences of blasting vibration effect, the buildings around the blasting zone may be damaged and cracked and may even collapse [1–3]. The degree of blasting vibration effect is closely related to characteristics of blasting vibration signals. Therefore, the study on the characteristics of blasting vibration signals is of great theoretical and practical significance for the prediction and control of blasting vibration effect. The peak particle velocity (PPV) is considered to be the most important parameter to represent the characteristics of blasting vibration signals. Many researchers have focused on developing empirical equations and statistical models for estimating PPV [4–8]. In the last few years, artificial intelligent (AI) methods have been widely employed for PPV prediction, such as artificial neural network (ANN) [9], support vector machine (SVM) [10–12], classification and regression tree (CART) [13], imperialistic competitive algorithm (ICA) [14], genetic algorithm (GA) [15, 16], particle swarm optimization (PSO) [17, 18], nested extreme learning machine (Nested-ELM) [19], and so on. In addition to PPV, dominant frequency is also considered as another important index to characterize blasting vibration signals, which has been studied by more and more scholars. Guo et al. [20], Zhou et al. [21], Peng et al. [22], and Gao et al. [23] analyzed the attenuation mechanism and attenuation law of dominant frequency of blasting vibration. Lu et al. [24], Li et al. [25], Liu et al. [26], and Gou et al. [27] proposed the theoretical formulas or prediction models with intelligent algorithms for dominant frequency.

Because of the very complex propagation mechanism and the strong randomness, fuzziness, and uncertainty of blasting vibration, the characteristics of blasting vibration

signals are quite different in different zones. Some researchers have tried to study the zoning method of blasting vibration and analyze signal characteristics in each zone. Li et al. [28], Pang and Chen [29], and Zhang et al. [30] took the different values of scaled charge or scaled distance as zoning indexes. Meng [31] and Wang [32] selected PPV as the threshold for blasting vibration zoning. The existing zoning indexes such as scaled charge, scaled distance, and PPV only reflect the intensity of blasting vibration signals or its main influence factors including the charge weight and distance from explosion source. Because of not considering the specific influences of geological and topographical conditions, the existing zoning methods of blasting vibration cannot fully describe the detailed characteristics of blasting vibration signals.

Support vector machine (SVM) is a very powerful multifunctional intelligent learning algorithm, which can perform linear or nonlinear regression, classification, and even outlier detection. And the SVM regression algorithm has been effectively applied in the prediction of blasting vibration intensity [10–12]. Because of keeping the original signal details, the time-domain signals can be used for characteristic extraction and classification with the help of appropriate algorithms [33–36]. Compared with other classification algorithms, the SVM classification algorithm has the advantages of relatively small sample demand, low structural risk, and nonlinearity [37], and it has been widely used in various fields [38–40]. Yang and Wu [41] used SVM classification algorithm to discriminate blasting vibration and rock fracture microseismic signals and achieved good classification results. However, how to identify and classify the detailed characteristics of the same blasting vibration signals in different zones remains to be further studied. Therefore, a new blasting vibration zoning method based on energy proportion was proposed in this paper. 343 sets of measured blasting vibration signals were selected for multiresolution wavelet analysis, and the energy distribution characteristics of each subfrequency band were studied. Then, using the proposed zoning method of blasting vibration based on energy proportion, the blasting vibration signals were divided into different blasting vibration zones. Finally, the zoning results were used as samples to train and test the SVM classification models with four different kernel functions. The testing results demonstrate that the new zoning method of blasting vibration based on energy proportion proposed in this paper has high feasibility, flexibility, and reliability, and the SVM classification models with RBF have high prediction accuracy.

The main contributions are given as follows:

(i) A new blasting vibration zoning method based on energy proportion was proposed, in which the energy proportion in low, medium, and high frequency band after multiresolution wavelet analysis is used as the zoning index to distinguish the different characteristics of blasting vibration signals in different zones.

(ii) 343 sets of measured blasting vibration signals were used to train and test the SVM classification models with four different kernel functions based on the proposed zoning method. The comparison results show that the SVM classification models with RBF have higher accuracy than models with other kernel functions in blasting vibration zoning prediction.

(iii) It is proved that the zoning method of blasting vibration based on energy proportion has high feasibility, flexibility, and reliability, and the SVM classification models with RBF have high prediction accuracy. The proposed zoning method and its SVM models can not only provide theoretical guidance for studying the specific characteristics of blasting vibration signals in each zone but also provide an important basis for the prediction, control, and safety standards for blasting vibration.

2. Classification Principle of SVM Algorithm

SVM is a machine learning method developed from statistical learning theory, and it has been widely used in solving various classification problems due to its excellent performance [42–45]. The classification principle of SVM algorithm is as follows [46–48].

It is assumed that the training sample set $\{(x_i, y_i), i = 1, 2, \ldots, l\}$ with size l consists of two categories to keep generality. When x_i is the first category, $y_i = 1$; when x_i is the second category, $y_i = -1$.

If the sample is linearly separable, there is a classification hyperplane:

$$wx + b = 0. \tag{1}$$

Then, make the sample set meet

$$\begin{cases} wx_i + b \geq 1, & y_i = 1, \\ wx_i + b \leq -1, & y_i = -1, \end{cases} \quad i = 1, 2, \ldots, l, \tag{2}$$

where w, x, $x_i \in R$, w, b, are the parameters to be determined; w is the normal vector of classification hyperplane $wx + b = 0$.

The margin between sample point x_i and classification hyperplane is defined as

$$\varepsilon_i = y_i (wx_i + b) = |wx_i + b|, \tag{3}$$

where w is normalized and defined as geometric margin:

$$\delta_i = \frac{wx_i + b}{\|w\|}. \tag{4}$$

In order to classify the sample set correctly, it is necessary to select an optimal classification hyperplane among the numerous classification hyperplanes to maximize the distance δ between the sample set and the classification hyperplane.

When $\varepsilon = |wx_i + b| = 1$, the distance between the two types of sample points is $2((|wx_i + b|)/\|w\|) = (2/\|w\|)$. And the goal is to find the optimal classification hyperplane under the constraint of formula (2) to make $(2/\|w\|)$ maximum and $(\|w\|^2/2)$ minimum.

Therefore, the linear separable SVM problem is transformed into a quadratic programming problem:

$$\begin{cases} \min \dfrac{1}{2}\|w\|^2, \\ \text{constraint condition:} \quad y_i((wx_i + b)) \geq 1, \quad i = 1, 2, \ldots, l. \end{cases} \tag{5}$$

Because the objective function and constraint condition are convex, according to the optimization theory, there is a unique global minimum solution to this problem. Use the Lagrange multiplier method and the KKT (Karush–Kuhn–Tucker) condition:

$$\alpha_i \left(y_i((xx_i) + b) - 1\right) = 0. \tag{6}$$

The optimal classification function can be obtained:

$$f(x) = \operatorname{sgn}\left[\sum_{i=1}^{l} \alpha_i^* y_i (xx_i) + b^*\right], \tag{7}$$

Table 1: Kernel functions in SVM models.

Types of kernel functions	Expressions
Linear kernel function(LKF)	$K(x, x_i) = xx_i$
Polynomial kernel function (PKF)	$K(x, x_i) = (xx_i + 1)^d$
Radial basis function (RBF)	$K(x, x_i) = \exp(-g \cdot \|x - x_i\|^2)$
Sigmoid kernel function (SKF)	$K(x, x_i) = \tanh(k(xx_i) + \theta)$

where sgn is the symbolic function, a^* and b^* are the parameters to determine the optimal hyperplane partition, and (xx_i) is the dot product of two vectors.

Most problems in engineering practice are nonlinear separable problems, and the quadratic programming problems can be modified as follows by introducing the slack variable ξ_i:

$$\begin{cases} \min \dfrac{1}{2}\|w\|^2 + C\sum_i \xi_i, \quad \xi_i \geq 0, \\ \text{constraint condition:} \ y_i((wx_i + b)) \geq 1 - \xi_i, \quad i = 1, 2, \ldots, l, \end{cases} \tag{8}$$

where ξ_i is the slack variable and C is the penalty coefficient.

Cortes and Vapnik [49] proposed that the kernel function $K(x_i, x_j)$ satisfying Mercer conditions should be used instead of dot product operations to solve duality problems:

$$K(x_i, x_j) = \Phi(x_i)\Phi(x_j). \tag{9}$$

And the optimal classification function is

$$\begin{aligned} f(x) &= \operatorname{sgn}(w^*\Phi(x) + b^*) = \operatorname{sgn}\left(\sum_{i=1}^{l} \alpha_i^* y_i \Phi(x_i) \cdot \Phi(x) + b^*\right) \\ &= \operatorname{sgn}\left(\sum_{i=1}^{l} \alpha_i^* y_i K(x_i, x) + b^*\right). \end{aligned} \tag{10}$$

The kernel functions commonly used in SVM models are shown in Table 1.

3. Proposal of a New Zoning Method of Blasting Vibration Based on Energy Proportion

3.1. Principle of Wavelet Analysis. Fourier analysis has solved many problems in signal processing. However, Fourier analysis can only obtain the whole spectrum of the signals, and it has shortcomings in analyzing local characteristics and processing time-varying nonstationary signals. Therefore, wavelet analysis [50], a new time-frequency analysis method, came into being. It retains the advantages of Fourier transform and makes up for the shortcomings in local analysis. Based on different wavelet functions [51], wavelet analysis can accurately reveal the distribution characteristics of signals in time and frequency domain simultaneously.

Meet the condition [52, 53]

$$\int_{-\infty}^{+\infty} |\Psi(\omega)|^2 |\omega|^{-1} \mathrm{d}\omega < 0, \tag{11}$$

where $\Psi(\omega)$ is the frequency-domain representation of the square integrable function $\phi(t)$ and $\phi(t)$ is a basic wavelet or wavelet function.

In the wavelet transform, the basic wavelet function first moves the displacement τ and then makes the inner product with the signal $X(t)$ in different scales of a:

$$WT_x(a, \tau) = \frac{1}{\sqrt{a}} \int_{-\infty}^{+\infty} x(t)\phi^*\left(\frac{t - \tau}{a}\right)\mathrm{d}t, \quad a > 0, \tag{12}$$

where a is the scale factor expanding or contracting with the basic wavelet function $\phi(t)$ and τ is the response displacement whose value can be positive or negative. Because both a and τ are continuous variables, the wavelet transform is also called continuous wavelet transform.

The equivalent frequency-domain representation of equation (12) is as follows:

$$WT_x(a, \tau) = \frac{\sqrt{a}}{2\pi} \int_{-\infty}^{+\infty} X(\omega)\Psi^*(a\omega)e^{+j\omega\tau}\mathrm{d}\omega, \tag{13}$$

where $X(\omega)$ is the frequency-domain representation of $x(t)$.

3.2. Multiresolution Wavelet Analysis of Blasting Vibration Signals. The blasting zone of groundwork excavation project in Rizhao District is about 260 m long and 120 m wide, and the excavation depth is 1–6 m. The geomorphic unit of the

site belongs to the low mountain or hilly area in the Yellow Sea land, and the geomorphic morphological type belongs to the structural denudation residual hill. The bedrock of the site is granite and gneiss, which forms different degrees of weathering zones from top to bottom because of experiencing a long period of geological process. The short-hole expanding blasting method is mainly adopted in the excavation project. The hole diameter is 38 mm, the hole spacing is about 1.2 m, the row spacing is 1 m, and the hole depth is 1.6 m.

In order to control the vibration effect caused by blasting excavation safely, the monitoring work of blasting vibration was carried out in the engineering site during the whole construction process. A large number of blasting vibration signals were measured by IDTS3850 blasting vibration testers and their matching speed sensors. Among them, 343 sets of effective typical signals in the same direction were selected as the sample data of signal identification and zoning in this paper.

The Sadovsky formula is deformed as follows:

$$v = K\left(\frac{r}{Q^{(1/3)}}\right)^{-\alpha}, \tag{14}$$

where v is PPV (cm/s), K and α are the coefficients related to blasting methods and site conditions, $(r/Q^{(1/3)})$ is the scaled distance (m/kg$^{1/3}$), r is the distance from explosion source (m), and Q is the maximum charge per delay (kg).

The zoning method of blasting vibration based on scaled distance in reference [54] is shown in Table 2.

Using the above zoning method, 343 sets of measured blasting vibration signals were divided into different blasting vibration zones. Then, the multiresolution wavelet analysis was carried out on the 343 sets of signals, and the wavelet basis function db8 of dbN wavelet system constructed by Inrid Daubechies was selected [55]. Because the sampling frequency of the blasting vibration testers used in this test is 10000 Hz, according to the sampling theorem, the Nyquist frequency is 10000/2 = 5000 Hz. Since the principle frequency of general buildings is in the range of 2~10 Hz, the blasting vibration signal at each measuring point is decomposed by wavelet with the scale of 11, and the corresponding 12 frequency bands are as follows: 0~2.441 Hz, 2.441~4.882 Hz, 4.882~9.765 Hz, 9.765~19.531 Hz, 19.531~39.062 Hz, 39.062~78.125 Hz, 78.125~156.25 Hz, 156.25~312.5 Hz, 312.5~625 Hz, 625~1250 Hz, 1250~2500 Hz, and 2500~5000 Hz.

Limited by the space, some sets of typical blasting vibration data in the near, medium, and far zones are listed here, as shown in Table 3. The dominant frequency, PPV, and energy proportion results of each subfrequency band of the signals listed in Table 3 by multiresolution wavelet analysis are shown in Tables 4–9.

3.3. A New Zoning Method of Blasting Vibration Based on Energy Proportion. It can be seen from Tables 4 to 6 that the zoning method of blasting vibration based on scaled distance basically conforms to the decay law of blasting vibration frequency: the frequency band of blasting vibration signals in the near zone is mainly high frequency band (≥78.125), the frequency band in the medium zone is mainly medium frequency band (9.7657~78.125), and the frequency band in the far zone is mainly low frequency band (0~9.7657). According to the blasting vibration zoning method based on scaled distance, signal 28 in Table 4 is divided into blasting vibration near zone, and the frequency is mainly in the high frequency band. Signal 57 in Table 5 is divided into medium zone, and the frequency is mainly in the medium frequency band. Signal 71 in Table 6 is divided into far zone, and the frequency is mainly in the low frequency band. The above zoning method effectively reflects the frequency decay characteristics of the near, medium, and far zones, which has a certain guiding role in studying the propagation law and characteristics of blasting vibration waves in different zones.

Table 2: Blasting vibration zoning method based on scaled distance.

$(r/Q^{(1/3)})$	Blasting vibration zones
$(0, 12)$	Blasting vibration near zone
$(12, 22)$	Blasting vibration medium zone
$(22, +\infty)$	Blasting vibration far zone

However, the limitations of the blasting vibration zoning method based on scaled distance are obvious. Tables 7 to 9 show the corresponding wavelet analysis results of blasting vibration signals selected separately from near, medium, and far zones based on scaled distance. Through observation, it can be seen that the frequency-band energy proportions of the signals in some blasting vibration zones show the characteristics of other zones, and the examples are as follows. Signal 10 in Table 7 is divided into blasting vibration near zone based on scaled distance; according to the decay law of blasting vibration frequency, the frequency in the near zone should be mainly in the high frequency band, but the dominant energy of the signal is mainly concentrated in the medium frequency band. Signal 6 in Table 8 is divided into blasting vibration medium zone based on scaled distance; according to the decay law of blasting vibration frequency, the frequency in the medium zone should be mainly in the medium frequency band, but the dominant energy of the signal is mainly concentrated in the low frequency band. Signal 5 in Table 9 is divided into blasting vibration far zone based on scaled distance; according to the decay law of blasting vibration frequency, the frequency in the far zone should be mainly in the low frequency band, but the dominant energy of the signal is mainly concentrated in the high frequency band. The existence of these special examples limits the study on the propagation characteristics of the blasting vibration signals in different zones and further affects the control of blasting vibration and the formulation of blasting safety standards.

Therefore, it is more reasonable to take the relative energy proportion of each frequency band as the index to divide blasting vibration zones, and a new zoning method of blasting vibration based on energy proportion was proposed in this paper, as shown in Figure 1.

The zoning method of blasting vibration based on energy proportion can be described as follows:

Table 3: Typical blasting vibration data in the near, medium, and far zones.

No.	Charge (kg)	Distance (m)	Scaled distance (m/kg$^{1/3}$)	Blasting vibration zone	PPV (cm/s)	Dominant frequency (Hz)
28	6.5	15	8.0375	Near zone	2.3444	323.4863
57	10	36.9	17.1275	Medium zone	0.8069	50.6592
71	11	63	28.3276	Far zone	0.0900	51.8799
10	20	26.9	9.9100	Near zone	0.6891	51.8799
6	9	35	16.8264	Medium zone	0.5264	222.1680
5	17.5	78.7	30.3130	Far zone	0.7203	42.7246

Table 4: Dominant frequency, PPV, and energy proportion of each subfrequency band at measuring point 28 in the near zone.

Frequency band (Hz)	Dominant frequency (Hz)	PPV (cm/s)	Energy proportion (%)
0~2.4415	1.8	0.0454	9.5090
2.4415~4.8829	3.7	0.0134	0.1108
4.8829~9.7657	6.1	0.0287	0.2129
9.7657~19.5313	12.8	0.0325	0.1905
19.5313~39.0625	28.1	0.0430	0.1714
39.0625~78.125	72	0.3041	2.9811
78.125~156.25	153.8	0.3302	1.9983
156.25~312.5	305.8	1.8699	64.5484
312.5~625	331.4	1.2202	19.7658
625~1250	919.2	0.2458	0.4337
1250~2500	1256.7	0.0841	0.0740
2500~5000	2774	0.0300	0.0040

Table 5: Dominant frequency, PPV, and energy proportion of each subfrequency band at measuring point 57 in the medium zone.

Frequency band (Hz)	Dominant frequency (Hz)	PPV (cm/s)	Energy proportion (%)
0~2.4415	0.6	0.0036	0.2496
2.4415~4.8829	4.3	0.0004	0.0005
4.8829~9.7657	7.3	0.0010	0.0016
9.7657~19.5313	15.3	0.0208	0.2916
19.5313~39.0625	38.5	0.2108	17.0179
39.0625~78.125	50.7	0.5771	79.6341
78.125~156.25	110.5	0.1483	2.5940
156.25~312.5	177.6	0.0358	0.1868
312.5~625	332.6	0.0114	0.0160
625~1250	748.3	0.0027	0.0029
1250~2500	2150.9	0.0026	0.0026
2500~5000	3251.3	0.0021	0.0024

Table 6: Dominant frequency, PPV, and energy proportion of each subfrequency band at measuring point 71 in the far zone.

Frequency band (Hz)	Dominant frequency (Hz)	PPV (cm/s)	Energy proportion (%)
0~2.4415	0.6	0.0453	97.8809
2.4415~4.8829	4.3	0.0005	0.0013
4.8829~9.7657	9.2	0.0005	0.0015
9.7657~19.5313	17.1	0.0043	0.0404
19.5313~39.0625	29.9	0.0224	0.5545
39.0625~78.125	51.3	0.0355	1.0447
78.125~156.25	80	0.0213	0.1552
156.25~312.5	235	0.0499	0.2468
312.5~625	355.2	0.0227	0.0561
625~1250	943	0.0079	0.0061
1250~2500	1761.5	0.0147	0.0071
2500~5000	2505.5	0.0176	0.0054

Table 7: Dominant frequency, PPV, and energy proportion of each subfrequency band at measuring point 10 in the near zone.

Frequency band (Hz)	Dominant frequency (Hz)	PPV (cm/s)	Energy proportion (%)
0~2.4415	2.4	0.0040	0.2963
2.4415~4.8829	2.4	0.0023	0.0132
4.8829~9.7657	8.5	0.0025	0.0242
9.7657~19.5313	17.7	0.0755	4.8651
19.5313~39.0625	36.6	0.2197	25.3723
39.0625~78.125	51.9	0.5305	66.5348
78.125~156.25	94.6	0.1026	2.8272
156.25~312.5	210.0	0.0130	0.0323
312.5~625	360.7	0.0060	0.0123
625~1250	731.2	0.0023	0.0090
1250~2500	1907.3	0.0025	0.0073
2500~5000	3092.7	0.0026	0.0059

Table 8: Dominant frequency, PPV, and energy proportion of each subfrequency band at measuring point 6 in the medium zone.

Frequency band (Hz)	Dominant frequency (Hz)	PPV (cm/s)	Energy proportion (%)
0~2.4415	1.2	0.0408	70.2143
2.4415~4.8829	3.7	0.0012	0.0072
4.8829~9.7657	7.9	0.0026	0.0153
9.7657~19.5313	14.0	0.0045	0.0193
19.5313~39.0625	25.0	0.0125	0.1006
39.0625~78.125	53.7	0.0780	1.5408
78.125~156.25	153.8	0.1529	4.6620
156.25~312.5	219.1	0.4386	17.6503
312.5~625	316.8	0.2489	5.5965
625~1250	752.0	0.0745	0.1226
1250~2500	2197.3	0.0291	0.0416
2500~5000	2802.7	0.0438	0.0295

Table 9: Dominant frequency, PPV, and energy proportion of each subfrequency band at measuring point 5 in the far zone.

Frequency band (Hz)	Dominant frequency (Hz)	PPV (cm/s)	Energy proportion (%)
0~2.4415	1.8	0.0030	0.2050
2.4415~4.8829	3.7	0.0019	0.0180
4.8829~9.7657	6.7	0.0019	0.0167
9.7657~19.5313	14.6	0.0064	0.0730
19.5313~39.0625	34.8	0.1199	12.3613
39.0625~78.125	48.8	0.1981	14.5865
78.125~156.25	121.5	0.2304	10.6664
156.25~312.5	227.7	0.5570	51.9499
312.5~625	330.8	0.2260	10.0215
625~1250	912.5	0.0082	0.0485
1250~2500	2269.9	0.0031	0.0337
2500~5000	2730.1	0.0038	0.0195

Step 1. Input the blasting vibration signal.

Step 2. Carry out multiresolution wavelet analysis on the blasting vibration signal.

Step 3. Obtain the energy proportion of each subfrequency band.

Step 4. Determine which zone the blasting vibration signal belongs to according to the following conditions. (1) When the energy proportion of high frequency band is higher than that of medium frequency band and low frequency band, the corresponding signal is divided into blasting vibration near zone. (2) When the energy proportion of medium frequency band is higher than that of high frequency band and low frequency band, the corresponding signal is divided into blasting vibration medium zone. (3) When the energy proportion of low frequency band is higher than that of high frequency band and medium frequency band, the corresponding signal is divided into blasting vibration far zone.

According to the zoning method of blasting vibration based on energy proportion, the frequency of signal 28 in Table 4 is mainly in the high frequency band, which is divided into blasting vibration near zone. The frequency of signal 57 in Table 5 is mainly in the medium frequency band, which is divided into blasting vibration medium zone. The frequency of signal 71 in Table 6 is mainly in the low frequency band, which is divided into blasting vibration far zone. The frequency of signal 10 in Table 7 is mainly in the medium frequency band, which is divided into blasting vibration medium zone. The frequency of signal 6 in Table 8 is mainly in the low frequency band, which is divided into blasting vibration far zone. The frequency of signal 5 in Table 9 is mainly in the high frequency band, which is divided into blasting vibration near zone.

4. SVM Classification Models of Blasting Vibration Zoning Method

Having enough samples with good typicality and high precision is an important condition for SVM modelling. 343 sets of representative effective signals were selected from a large number of measured blasting vibration signals, and the results by wavelet multiresolution analysis were taken as samples of SVM classification models. Table 10 shows the energy proportion results of 343 sets of measured blasting vibration signals after multiresolution wavelet analysis and the classification results by the

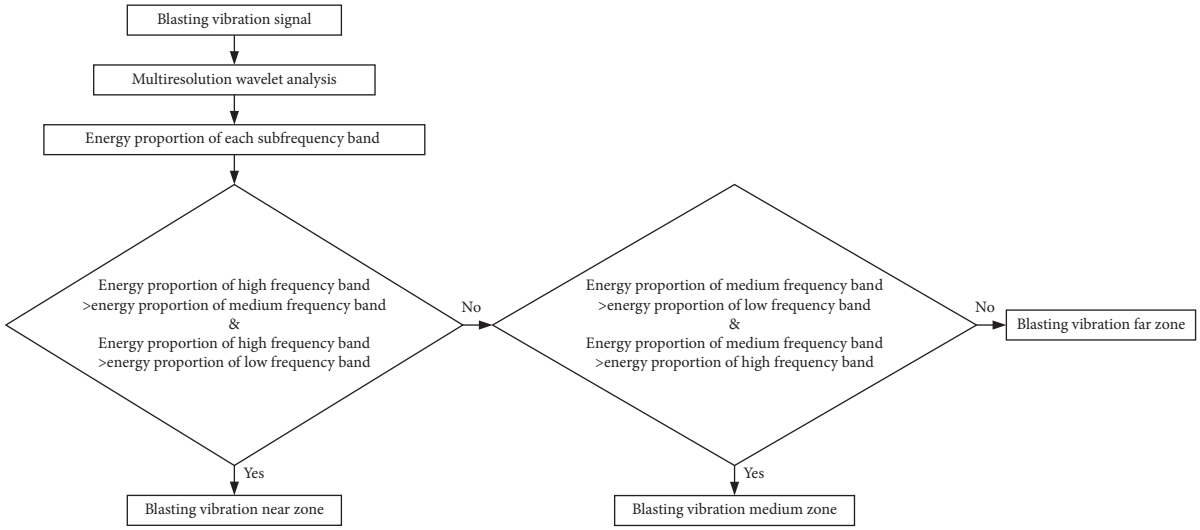

Figure 1: Flowchart of the zoning method of blasting vibration based on energy proportion.

blasting vibration zoning method proposed in Section 3.3. Labels 1 to 3 represent blasting vibration near, medium, and far zones, respectively.

Using simple random sampling method, 257 sets of samples (75% of the total number of samples) in Table 10 were selected as training samples of SVM classification models and the SVM classification models were established. Among the 257 sets of training samples, there are 28 sets of samples in the near zone, 195 sets of samples in the medium zone, and 34 sets of samples in the far zone. The remaining 86 sets of samples (25% of the total number of samples) were taken as testing samples to verify the established models. Among the 86 sets of testing samples, there are 28 sets of samples in the near zone, 45 sets of samples in the medium zone, and 13 sets of samples in the far zone. As shown in Table 10, samples 1 to 257 are training samples, and samples 258 to 343 are testing samples.

In order to reduce the influence of the large difference between the parameters of the samples on the performance of prediction models, all sample data should be normalized according to the following formula before the training of SVM classification models [56]:

$$X_{ij} = \frac{2\left(x_{ij} - x_{\min}(i)\right)}{x_{\max}(i) - x_{\min}(i)} - 1, \tag{15}$$

where x_{ij} is the measured value of the ith variable in the jth sample and $x_{\max}(i)$ and $x_{\min}(i)$are the maximum and minimum measured values of the ith variables.

All the sample data in Table 10 were normalized to [−1, 1] by formula (15). After the classification of the models was completed, the classification results were also anti-normalized by using this formula.

Four types of kernel functions including LKF, PKF, RBF, and SKF were used to train SVM classification models, and different parameters were selected by the cross validation method for SVM classification models with any type of kernel function. Then, the optimal parameters were obtained for training models, and the blasting vibration zoning models based on energy proportion were established.

The accuracy of SVM classification models is evaluated by the following formula:

$$\text{accuracy} = \frac{N_c}{N_t} \times 100\%, \tag{16}$$

where N_c is number of samples correctly classified and N_t is total number of samples.

The flowchart of SVM classification models of the proposed blasting vibration zoning method in this paper is shown in Figure 2.

The detailed steps of SVM classification models are as follows:

Step 1. The data are normalized and divided into training samples and testing samples.

Step 2. Initialize the parameters of SVM classification models, which include penalty coefficient and kernel function parameters.

Step 3. Optimize the penalty coefficient and kernel parameters. In SVM training, the penalty coefficient and kernel function parameters take discrete values in a certain range, and then the optimal values with the highest accuracy are obtained by the cross validation method.

Step 4. The optimal parameters obtained in Step 3 are used as the parameters of SVM classification models to classify the testing samples. If the end conditions are met, the SVM classification models and the classification accuracy are saved. Otherwise, return to Step 3.

Step 5. Output the SVM classification models with four kernel functions and their classification accuracy.

The parameters and accuracy of SVM classification models with four kernel functions based on the 343 sets of samples are shown in Table 11.

It can be seen from Table 11 that the average values of classification accuracy of SVM models with LKF, PKF, RBF,

Table 10: Samples of SVM classification models.

No.	PD1	PD2	PD3	PD4	PD5	PD6	PD7	PD8	PD9	PD10	PD11	PD12	Types
1	34.9899	0.0006	0.0053	0.0837	4.6407	55.7647	3.5752	0.7976	0.1192	0.0087	0.0086	0.0057	2
2	0.4266	0.0057	0.0325	0.9285	5.0815	69.3728	22.8396	1.282	0.0199	0.0039	0.0038	0.0033	2
3	10.1402	0.0009	0.0036	0.3908	10.61	69.7286	8.7192	0.3669	0.0357	0.0014	0.0015	0.0013	2
4	49.9183	0.0017	0.0049	0.3082	6.5566	32.9399	9.4449	0.7546	0.0362	0.0134	0.0132	0.0081	3
5	0.669	0.3257	0.3221	0.3979	0.9096	19.9203	49.1775	8.13	15.3682	2.0379	2.6942	0.0477	1
6	5.3003	0.0229	0.4616	1.1009	2.7226	25.3614	10.2591	40.1265	14.2514	0.2683	0.1195	0.0056	1
7	20.8464	0.4202	0.4336	0.4739	0.2685	0.8827	4.3216	15.2323	56.4006	0.4078	0.3068	0.0055	1
8	0.2394	0.0056	0.1217	0.8419	16.961	77.2803	4.4831	0.0613	0.0025	0.001	0.0011	0.0011	2
9	3.552	1.4435	0.9823	2.4488	20.0208	34.9933	32.1278	2.9461	0.8424	0.3046	0.123	0.2153	2
10	1.2521	0.8527	0.6572	0.3043	0.7247	2.9896	35.9766	33.3059	19.3597	3.0272	1.5348	0.0152	1
11	19.5308	0.22	0.3121	0.1818	0.2147	0.7938	0.8867	34.9105	41.4989	0.9115	0.5299	0.0093	1
12	0.0423	0.002	0.0051	0.6367	4.7189	84.4154	10.1338	0.0437	0.0006	0.0005	0.0005	0.0005	2
13	9.5117	0.0009	0.0031	0.9062	70.0943	18.7993	0.6401	0.0257	0.0064	0.0042	0.0042	0.0038	2
14	9.9489	0.0012	0.0978	0.6183	28.6976	58.4203	2.1463	0.0408	0.0102	0.0073	0.0059	0.0053	2
15	0.2728	0.0038	0.1004	0.5473	13.5466	80.2582	5.2088	0.0574	0.0017	0.0009	0.001	0.001	2
...	...	...	...	...	...	...	...	...	...	...	...	...	...
329	45.168	0.0029	0.112	0.3264	15.502	20.2044	16.4387	2.0677	0.1224	0.0257	0.0167	0.0133	3
330	1.2114	0.017	0.0515	0.3248	10.7671	45.9149	40.0368	1.5904	0.0439	0.0175	0.014	0.0108	2
331	65.8766	0.0094	0.0163	0.1364	6.6911	13.4421	11.9669	1.2144	0.5079	0.0615	0.0417	0.0358	3
332	0.2774	0.0207	0.0791	0.1799	8.379	67.579	22.7869	0.6862	0.005	0.0025	0.002	0.0022	2
333	13.1182	0.0008	0.0144	0.0923	16.8056	59.9594	8.3206	1.612	0.0538	0.0095	0.0075	0.0059	2
334	0.4644	0.0267	0.1362	0.9169	5.8446	72.4972	19.0858	1.0113	0.0067	0.0036	0.0032	0.0034	2
335	23.3669	0.001	0.0079	1.3397	21.1059	34.2772	17.7088	2.0573	0.0974	0.0166	0.0119	0.0093	2
336	0.9944	0.0034	0.1349	1.4361	8.5149	51.1464	36.9286	0.7893	0.0194	0.0119	0.0123	0.0083	2
337	12.0654	0.0007	0.0019	0.2775	11.6415	71.6843	4.0703	0.2333	0.021	0.0014	0.0015	0.0013	2
338	76.8729	0.0027	0.0203	0.1738	4.5146	12.6639	5.4112	0.2615	0.0361	0.0157	0.0163	0.011	3
339	1.7324	0.0013	0.0571	0.3428	1.4073	84.1498	10.6934	1.519	0.0651	0.0111	0.0112	0.0095	2
340	26.6758	0.0012	0.0165	0.2755	18.7241	46.8901	6.8235	0.5219	0.0629	0.0027	0.0031	0.0027	2
341	85.1141	0.0011	0.0043	0.0881	2.8739	7.9185	3.4547	0.406	0.0724	0.0264	0.0252	0.0153	3
342	0.2431	0.0013	0.0351	0.204	5.1819	83.2178	9.4493	1.6365	0.0255	0.0018	0.002	0.0017	2
343	8.4562	0.0004	0.003	0.0743	7.5993	74.9625	8.3907	0.4444	0.0654	0.0014	0.0013	0.0012	2

Note. PD1~PD12, respectively, represent frequency bands of 0~2.441 Hz, 2.441~4.882 Hz, 4.882~9.765 Hz, 9.765~19.531 Hz, 19.531~39.062 Hz, 39.062~78.125 Hz, 78.125~156.25 Hz, 156.25~312.5 Hz, 312.5~625 Hz, 625~1250 Hz, 1250~2500 Hz, and 2500~5000 Hz.

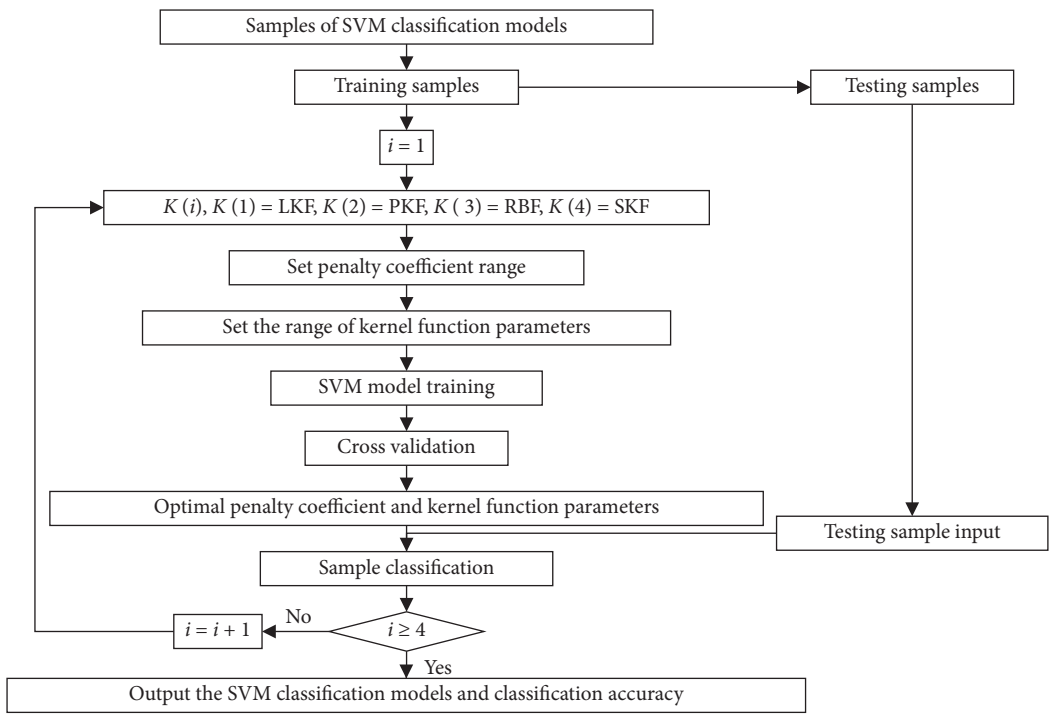

Figure 2: Flowchart of SVM classification models.

Table 11: Parameters and prediction accuracy of SVM classification models with different kernel functions.

No.	Kernel functions			SVM classification models					
	Types	Parameters	Values	c	Iterations	Number of support vectors	Accuracy of training samples	Accuracy of testing samples	Average values of prediction accuracy
1	LKF	—	—	4.5948	35	35	99.2218	97.6744	97.7907
2				48.5029	92	20	100	96.5116	
3				8	40	29	99.2218	97.6744	
4				13.9288	92	26	100	97.6744	
5				6.9644	41	30	99.2218	97.6744	
6				24.2515	92	22	100	98.8372	
7				21.1121	92	23	100	98.8372	
8				10.5561	76	29	99.6109	97.6744	
9				4	35	35	99.2218	97.6744	
10				6.0629	46	31	99.2218	97.6744	
11	PKF	d	1	0.0045	28	114	75.8755	53.3256	92.1930
12			2	4	82	21	100	96.5116	
13			3	27.8576	48	21	100	97.6744	
14			4	32	24	22	100	97.6744	
15			5	42.2243	24	22	100	96.5116	
16			6	36.7583	22	23	100	95.3488	
17			7	32	21	23	100	95.3488	
18			8	42.2243	20	25	100	96.5116	
19			9	42.2243	17	26	100	96.5116	
20			10	55.7152	17	28	100	96.5116	
21	RBF	g	0.1649	27.8576	54	33	99.2218	98.8372	98.7209
22			0.0625	73.5167	35	30	99.2218	98.8372	
23			0.0947	24.2515	31	35	99.2218	98.8372	
24			0.1250	21.1121	37	36	99.2218	98.8372	
25			0.1088	32	32	32	99.2218	98.8372	
26			0.1436	32	47	33	99.2218	98.8372	
27			0.1250	27.8576	33	34	99.2218	98.8372	
28			0.1436	48.5029	137	32	100	98.8372	
29			0.1649	21.1121	39	34	99.6109	98.8372	
30			0.0136	168.8970	34	35	99.2218	97.6744	
31	SKF	k	0.0825	84.4485	35	35	99.2218	97.6744	97.7907
32			0.0625	97.0059	25	35	99.2218	97.6744	
33			0.0947	445.7219	75	24	100	98.8372	
34			0.0718	168.8970	43	28	99.2218	97.6744	
35			0.0825	168.8970	60	29	99.2218	97.6744	
36			0.0421	675.5881	68	22	100	98.8372	
37			0.0825	388.0234	80	24	100	97.6744	
38			0.0947	222.8609	54	26	99.6109	97.6744	
39			0.1895	36.7583	48	51	99.2218	96.5116	
40			0.0272	168.8970	25	35	99.2218	97.6744	

and SKF are 97.7907%, 92.1930%, 98.7209%, and 97.7907%, respectively, among which the accuracy of SVM model with RBF is the highest. Based on the SVM classification models with RBF of Nos. 21 to 27, the accuracy to classify the training samples is 99.2218% and the accuracy to classify the testing samples is 98.8372%. Based on the SVM classification model with RBF of No. 28, the accuracy to classify the training samples is 100% and the accuracy to classify the testing samples is 98.8372%. Based on the SVM classification model with RBF of No. 29, the accuracy to classify the training samples is 99.6109% and the accuracy to classify the testing samples is 98.8372%. Based on the SVM classification model with RBF of No. 30, the accuracy to classify the training samples is 99.2218% and the accuracy to classify the testing samples is 97.6744%. All the SVM classification models with RBF of different parameters selected by the cross validation method show good prediction effect in blasting vibration zoning prediction, and the prediction accuracy of all the SVM models with RBF is more than 97.5% without overfitting. The classification results show that the zoning method of blasting vibration based on energy proportion proposed in this paper has high feasibility, flexibility, and reliability, and the classification algorithm of SVM models with RBF has high accuracy in blasting vibration zoning prediction.

The prediction results of testing samples by SVM classification models with RBF of Nos. 21 to 29 in Table 11 are shown in Figure 3, and the prediction results of testing samples by SVM classification model with RBF of No. 30 in Table 11 are shown in Figure 4. It can be found that all the

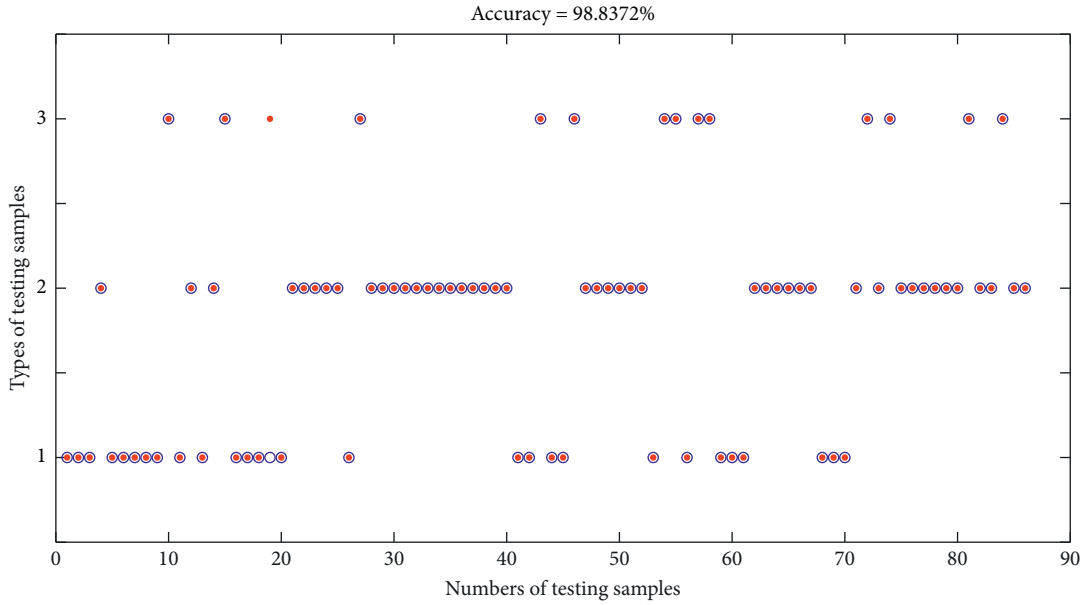

Figure 3: Prediction results of testing samples by SVM classification models of Nos. 21 to 29.

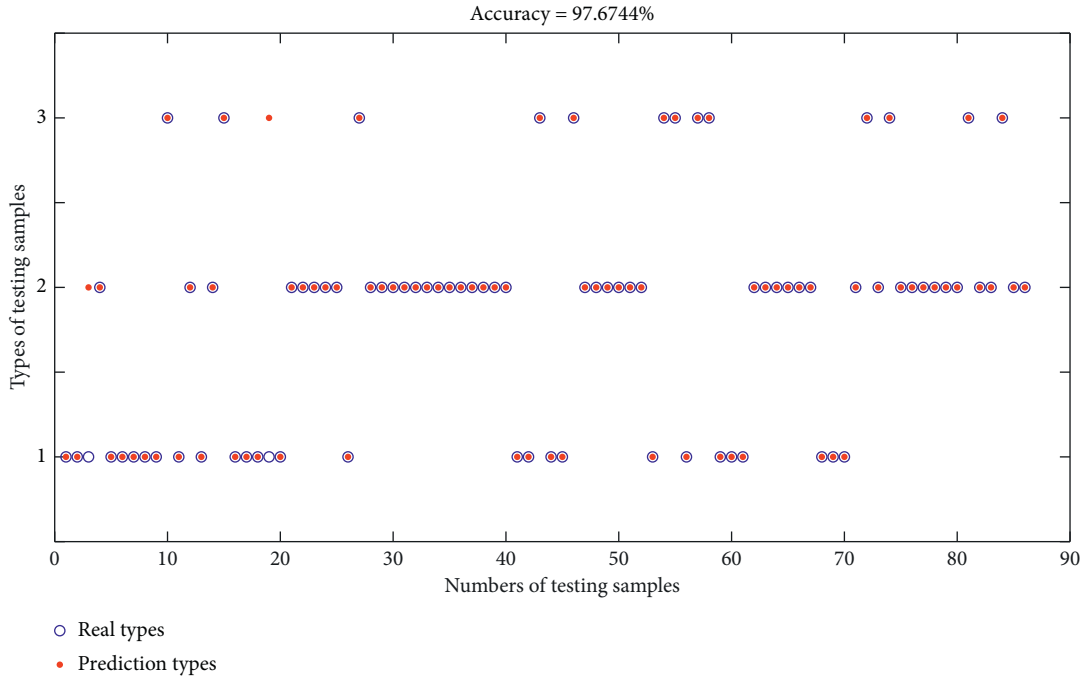

Figure 4: Prediction results of testing samples by SVM classification model of No. 30.

SVM classification models with RBF of Nos. 21 to 30 of different parameters in Table 11 classify sample 19 (corresponding to sample 276 in Table 10) incorrectly, and the SVM classification model with RBF of No. 30 classifies sample 3 (corresponding to sample 260 in Table 10) incorrectly. The energy proportions of sample 19 in frequency band 0~2.4415 Hz (43.6350%) and sample 3 in frequency band 39.062~78.125 Hz (28.3373%) are both more than 10%. It is considered that the energy proportion of the two frequency bands cannot be ignored according to reference [57]. Therefore, the SVM classification models with RBF cannot identify and classify samples 19 and 3 correctly, which reflects the influence of sample typicality on the prediction effect of the SVM classification algorithm.

5. Conclusions

The automatic identification and classification of blasting vibration signals in different zones is a complex subject, which is a powerful means to study the detailed characteristics for blasting vibration signals. Because of not considering the specific influences of geological and topographical conditions, the existing zoning methods for blasting vibration have some limitations. In this study, a new blasting vibration zoning method based on energy proportion was proposed. The energy proportion characteristics of each subfrequency band were extracted by multiresolution wavelet analysis, and the blasting vibration near, medium, and far zones were divided corresponding to the dominant energy proportion of high, medium, and low frequency bands.

Based on the proposed zoning method, 257 sets of measured blasting vibration signals were selected as training samples and 86 sets were selected as testing samples to train and test the SVM classification models with four different kernel functions of LKF, PKF, RBF, and SKF. All the SVM classification models with RBF of different parameters selected by the cross validation method show good prediction effect in blasting vibration zoning prediction, and the prediction accuracy of all the SVM models with RBF is more than 97.5% without overfitting. It is proved that the zoning method of blasting vibration based on energy proportion proposed in this paper has high feasibility, flexibility, and reliability, and the SVM classification models with RBF have high prediction accuracy.

However, there may be some mistakes in the classification of atypical signals when the number of signal samples in some blasting vibration zones is relatively small [58] and the energy proportion of signals in other frequency band is more than 10%. As in this paper, because there are more samples in the medium zone than those in the near and far zones, SVM classification models are very good for the classification of atypical signals in the medium zone, and even the accuracy is 100%. Therefore, in the future work, we can increase the number of signal samples in the near and far zones to enhance the identification ability of SVM classification models for atypical signals and further improve the classification accuracy.

The frequency bands of the near, medium, and far zones by the proposed zoning method of blasting vibration based on energy proportion are basically in accordance with the frequency bands of blasting vibration safety standard in "*blasting safety regulations*" [59]: (0, 10), (10, 50), (50, 100). Therefore, the zoning method can not only provide theoretical guidance for studying the specific characteristics of blasting vibration signals in each vibration zone but also provide an important basis for the prediction, control, and safety standards for blasting vibration.

Data Availability

The data used to support the findings of this study are included within the article.

Conflicts of Interest

The authors declare that there are no conflicts of interest regarding the publication of this paper.

Acknowledgments

This study was supported by the National Natural Science Foundation of China (nos. 51874123 and 51504082) and the Open Project Foundation of Fujian Research Center for Tunneling and Urban Underground Space Engineering (no. 16FTUE01).

References

[1] M. Khandelwal and M. Saadat, "A dimensional analysis approach to study blast-induced ground vibration," *Rock Mechanics and Rock Engineering*, vol. 48, no. 4, pp. 727–735, 2015.

[2] A. Sołtys, M. Twardosz, and J. Winzer, "Control and documentation studies of the impact of blasting on buildings in the surroundings of open pit mines," *Journal of Sustainable Mining*, vol. 16, no. 4, pp. 179–188, 2017.

[3] T. Wang, Z. Song, J. Yang et al., "Experimental research on dynamic response of red sandstone soil under impact loads," *Geomechanics and Engineering*, vol. 17, no. 4, pp. 393–403, 2019.

[4] M. Monjezi, M. Baghestani, R. Shirani Faradonbeh et al., "Modification and prediction of blast-induced ground vibrations based on both empirical and computational techniques," *Engineering with Computers*, vol. 32, no. 2, pp. 717–728, 2016.

[5] G. Liu, "Prediction of blasting vibration velocity for large-section tunnel blasting," *Blasting*, vol. 36, no. 3, pp. 129–136, 2019.

[6] H. Aawal and A. K. Mishra, "Modified scaled distance regression analysis approach for prediction of blast-induced ground vibration in multi-hole blasting," *Journal of Rock Mechanics and Geotechnical Engineering*, vol. 11, no. 1, pp. 202–207, 2019.

[7] V. K. Himanshu, M. P. Roy, A. K. Mishra et al., "Multivariate statistical analysis approach for prediction of blast-induced ground vibration," *Arabian Journal of Geosciences*, vol. 11, no. 16, 11 pages, Article ID 460, 2018.

[8] M. I. Matidza, Z. Jianhua, H. Gang, and A. D. Mwangi, "Assessment of blast-induced ground vibration at jinduicheng molybdenum open pit mine," *Natural Resources Research*, vol. 29, no. 2, pp. 831–841, 2020.

[9] M. Monjezi, M. Ghafurikalajahi, and A. Bahrami, "Prediction of blast-induced ground vibration using artificial neural networks," *Tunnelling and Underground Space Technology*, vol. 26, no. 1, pp. 46–50, 2011.

[10] M. Hasanipanah, M. Monjezi, A. Shahnazar, D. Jahed Armaghani, and A. Farazmand, "Feasibility of indirect determination of blast induced ground vibration based on support vector machine," *Measurement*, vol. 75, pp. 289–297, 2015.

[11] B. Mei, X. Wang, and R. Yang, "Prediction of blasting vibration intensity based on adaboost-SVM combination algorithm," *Journal of Vibration and Shock*, vol. 38, no. 18, pp. 231–235, 2019.

[12] Q. Yuan, S. Zhai, L. Wu, P. Chen, Y. Zhou, and Q. Zuo, "Blasting vibration velocity prediction based on least squares

support vector machine with particle swarm optimization algorithm," *Geosystem Engineering*, vol. 22, no. 5, pp. 279–288, 2019.

[13] M. Hasanipanah, R. S. Faradonbeh, H. B. Amnieh, D. J. Armaghani, and M. Monjezi, "Forecasting blast-induced ground vibration developing a CART model," *Engineering with Computers*, vol. 33, no. 2, pp. 307–316, 2017.

[14] M. Hasanipanah, H. Bakhshandeh Amnieh, H. Khamesi, D. Jahed Armaghani, S. Bagheri Golzar, and A. Shahnazar, "Prediction of an environmental issue of mine blasting: an imperialistic competitive algorithm-based fuzzy system," *International Journal of Environmental Science and Technology*, vol. 15, no. 3, pp. 551–560, 2018.

[15] E. Tian, J. Zhang, M. Soltani Tehrani, A. Surendar, and A. Z. Ibatova, "Development of GA-based models for simulating the ground vibration in mine blasting," *Engineering with Computers*, vol. 35, no. 3, pp. 849–855, 2019.

[16] M. Hasanipanah, S. B. Golzar, I. A. Larki, M. Y. Maryaki, and T. Ghahremanians, "Estimation of blast-induced ground vibration through a soft computing framework," *Engineering with Computers*, vol. 33, no. 4, pp. 951–959, 2017.

[17] H. Eskandar, E. Heydari, M. Hasanipanah, M. Jalil Masir, and A. Mahmodi Derakhsh, "Feasibility of particle swarm optimization and multiple regression for the prediction of an environmental issue of mine blasting," *Engineering Computations*, vol. 35, no. 1, pp. 363–376, 2018.

[18] X. Bui, P. Jaroonpattanapong, H. Nguyen et al., "A novel hybrid model for predicting blast-induced ground vibration based on *k*-nearest neighbors and particle swarm optimization," *ScientificReports*, vol. 9, no. 1, 14 pages, Article ID 13971, 2019.

[19] H. Wei, J. Chen, J. Zhu, X. Yang, and H. Chu, "A novel algorithm of nested-ELM for predicting blasting vibration," *Engineering with Computers*, 2020.

[20] T. Guo, X. Fang, Q. Xie et al., "Application of FSWT in accurate extraction of time-frequency features for blasting vibration signals," *Journal of Vibration and Shock*, vol. 32, no. 22, pp. 73–78, 2013.

[21] J. Zhou, W. Lu, L. Zhang et al., "Attenuation of vibration frequency during propagation of blasting seismic wave," *Chinese Journal of Rock Mechanics and Engineering*, vol. 33, no. 11, pp. 2171–2178, 2014.

[22] Y. Peng, Y. Su, L. Wu et al., "Study on the attenuation characteristics of seismic wave energy induced by underwater drilling and blasting," *Shock and Vibration*, vol. 2019, Article ID 4367698, 13 pages, 2019.

[23] Q. Gao, W. Lu, Z. Leng et al., "Effect of initiation location within blast hole on blast vibration field and its mechanism," *Shock and Vibration*, vol. 2019, Article ID 5386014, 18 pages, 2019.

[24] W. Lu, J. Zhou, M. Chen et al., "Study on attenuation formula of dominant frequency of blasting vibration," *Engineering Blasting*, vol. 21, no. 6, 6 pages, 2015.

[25] H. Li, X. Li, J. Li, X. Xia, and X. Wang, "Application of coupled analysis methods for prediction of blast-induced dominant vibration frequency," *Earthquake Engineering and Engineering Vibration*, vol. 15, no. 1, pp. 153–162, 2016.

[26] D. Liu, W. Lu, Y. Liu et al., "Analysis of the main factors influencing the dominant frequency of blast vibration," *Shock and Vibration*, vol. 2019, Article ID 8480905, 17 pages, 2019.

[27] Y. Gou, X. Shi, J. Zhou et al., "Attenuation assessment of blast-induced vibrations derived from an underground mine," *International Journal of Rock Mechanics and Mining Sciences*, vol. 127, p. 13, Article ID 104220, 2020.

[28] B. Li, "Vibration effect of longhole blasting in open pit mining," *Mining Research and Development*, vol. 9, no. 4, pp. 84–94, 1989.

[29] H. Pang and S. Chen, "Variation law of blasting seismic wave's propagation in elastic media," *Journal of Vibration and Shock*, vol. 28, no. 3, pp. 105–107, 2009.

[30] Z. Zhang, C. Lin, Z. Huang et al., "Prediction of blasting vibration of area near tunnel blasting source," *Explosion and Shock Waves*, vol. 34, no. 3, pp. 367–372, 2014.

[31] D. Meng, *Study on Construction Blasting Vibration Influence and Partition in Railway Interchange Tunnel*, Central South University, Changsha, China, 2014.

[32] H. Wang, *Study on Blasting Vibration Propagation and Partition in Super Large Section Small Spacing Tunnel*, Southwest Jiaotong University, Chengdu, China, 2019.

[33] Z. Du, R. Zhang, and H. Chen, "Characteristic signal extracted from a continuous time signal on the aspect of frequency domain," *Chinese Physics B*, vol. 28, Article ID 090502, 7 pages, 2019.

[34] W. Deng, H. Liu, J. Xu, H. Zhao, and Y. Song, "An improved quantum-inspired differential evolution algorithm for deep belief network," *IEEE Transactions on Instrumentation and Measurement*, vol. 69, no. 10, pp. 7319–7327, 2020.

[35] Y. Song, D. Wu, W. Deng et al., "MPPCEDE: multi-population parallel co-evolutionary differential evolution for parameter optimization," *Energy Conversion and Management*, vol. 228, Article ID 113661, 19 pages, 2021.

[36] Y. Song, D. Wu, A. Mohamed et al., "Enhanced success history adaptive DE for parameter optimization of photovoltaic models," *Complexity*, vol. 2021, Article ID 6660115, 2021.

[37] "Classification algorithm SVM (support vector machine)," 2020, https://blog.csdn.net/dcrmg/article/details/53000150.

[38] X. Wang, S. Yan, D. Li et al., "Pedestrian navigation nero-speed correction method based on support vector machine classification decision," *Science Technology and Engineering*, vol. 19, no. 1, pp. 159–165, 2019.

[39] S. Solikin, H. Manik, S. Pujiyati et al., "Support vector machine classification method for predicting Jakarta Bay bottom sediment type using multibeam echosounder data," *Pertanika Journal of Science and Technology*, vol. 48, no. 2, pp. 477–491, 2020.

[40] L. Tang, M. Zhang, and L. Wen, "Support vector machine classification of seismic events in the Tianshan orogenic belt," *Journal of Geophysical Research: Solid Earth*, vol. 125, no. 1, 2020.

[41] C. Yang and J. Wu, "Discriminating blasting vibration and rock fracture micro-seismic signal based on wavelet packet analysis and SVM," *Bulletin of Science and Technology*, vol. 35, no. 1, pp. 19–23, 2019.

[42] V. Vapnik, *Statistical Learning Theory*, John Wiley & Sons Inc, New York, NY, USA, 1998.

[43] V. Vapnik, *The Nature of Statistical Learning Theory*, Springer-Verlag, New York, NY, USA, 2000.

[44] N. Cristianini and J. Shawa-Taylor, *An Introduction of Support Vector Machines and Other Kernel-Based Learning Methods*, Cambridge University Press, Cambridge, UK, 2000.

[45] C. J. C. Burges, "A tutorial on support vector machines for pattern recognition," *Data Mining and Knowledge Discovery*, vol. 2, no. 2, pp. 121–167, 1998.

[46] Y. Chen, X. Yu, X. Gao et al., "A new method for non-linear classify and non-linear regression I: introduction to support

vector machine," *Journal of Applied Meteorological Science*, vol. 15, no. 3, pp. 345–354, 2004.

[47] W. Lu, N. Chen, C. Ye et al., "Introduction to the algorithm of support vector machine and the software Chem SVM," *Computers and Applied Chemistry*, vol. 19, no. 6, pp. 697–702, 2002.

[48] L. Yu, *30 Cases Analysis of MATLAB Intelligent Algorithm*, Beijing University Press, Beijing, China, 2011.

[49] C. Cortes and V. Vapnik, "Support-vector networks," *Machine Learning*, vol. 20, no. 3, pp. 273–297, 1995.

[50] I. Daubechies, "Orthonormal bases of compactly supported wavelets," *Communications on Pure and Applied Mathematics*, vol. 41, no. 7, pp. 909–996, 1988.

[51] Y. Sun and D. Liu, "Time-frequency analysis and wavelet transform and their applications," *Engineering Journal of Wuhan University*, vol. 36, no. 2, pp. 103–106, 2003.

[52] S. Li, "Wavelet transform and applications," *Progress in Geophysics*, vol. 7, no. 2, pp. 45–53, 1992.

[53] J. Wang, M. Wu, and Y. Sun, "Wavelet transform and applications," *Journal of Henan Normal University*, vol. 30, no. 2, pp. 86–89, 2002.

[54] S. Chen, H. Wei, and R. Du, "Multi-resolution wavelet analysis of blasting vibration signals," *Rock and Soil Mechanics*, vol. 30, no. s1, pp. 135–139, 2009.

[55] T. Liu, X. Zeng, and J. Zeng, *Introduction to Practical Wavelet Analysis*, National Defense Industry Press, Beijing, China, 2006.

[56] E. M. Golafshani and A. Ashour, "A feasibility study of BBP for predicting shear capacity of FRP reinforced concrete beams without stirrups," *Advances in Engineering Software*, vol. 97, pp. 29–39, 2016.

[57] Intellectual Property Publishing House, *CN201811310006.3 Method for Constructing Blasting Seismic Wave Model Equivalent Based on Building Earthquake Response*, Intellectual Property Publishing House, Beijing, China, 2019.

[58] J. Zhou, E. Li, H. Wei et al., "Random forests and cubist algorithms for predicting shear strengths of rockfill materials," *Applied Sciences*, vol. 9, no. 8, 16 pages, Article ID 9081621, 2019.

[59] Standardization Administration of China, *Chinese National Standard GB6722-2014: Safety Regulation for Blasting*, Standardization Administration of China, Beijing, China, 2014.